

FABRICATION OF SUB-MICRON STRUCTURES WITH HIGH ASPECT RATIO FOR MEMS USING DEEP X-RAY LITHOGRAPHY

Hiroshi Ueno, Nobuyoshi Nishi and Susumu Sugiyama

Faculty of Science and Engineering, Ritsumeikan University

1-1-1 Noji-Higashi, Kusatsu, Shiga 525-8577, Japan

phone: +81-77-561-2845, facsimile: +81-77-561-2845, e-mail: sme20034@se.ritsumei.ac.jp

ABSTRACT

In this paper, we present the fabrication of sub-micron structures with high aspect ratio for practical and high performance microelectromechanical systems (MEMS) using deep X-ray lithography. It is necessary for practical and high performance MEMS to be fabricated microstructures with sub-micron widths and gaps (lines and spaces). In order to fabricate the sub-micron microstructures, sub-micron deep X-ray lithography has been investigated. As a result, a sub-micron PMMA structure with 0.2 μm minimum width, 6 μm length and 17 μm height was fabricated by deep X-ray lithography using an X-ray mask with thick X-ray absorbers having sub-micron width.

INTRODUCTION

In the microelectromechanical system (MEMS) field, microstructures with high aspect ratio fabricated by the LIGA process, deep RIE and so on, are attracting attention because the microstructures are expected to be applied to high power microactuators driven by low voltage, and to high sensitivity microsensors. As the results of our previous work using the LIGA process show, microstructures with aspect ratio of 100, corresponding to 2 μm width and 200 μm height, were fabricated [1] and actuation of a wobble motor with aspect ratio of 50, corresponding to a 2 μm minimum gap and 100 μm height, was confirmed [2]. The results of another study reported that microstructures with the feature size of 1 μm width and 100 μm height were able to be fabricated [3].

It is necessary that microstructures with sub-micron widths and gaps (lines and spaces) be fabricated for practical and high performance MEMS for the following reasons: Microstructures with gaps less than 0.2 μm can decrease driving voltage of electrostatic micro-actuators to less than 15V [2,4]. Microstructures with widths and gaps (lines and spaces) less than 0.2 μm can be applied to Bragg grating having $\lambda/4$ pitch of visible light for optical communication devices.

In this paper, we present the fabrication of sub-micron structures with high aspect ratio for practical and high performance MEMS using deep X-ray lithography.

RESOLUTION

Fresnel diffraction and the creation of photoelectrons are important factors having influence on the resolution of X-ray lithography [5]. The influence of Fresnel diffraction will be increased at longer wavelengths. The resolution limit caused by Fresnel diffraction, R_d , is given by

$$R_d = 1.5(\lambda \cdot G / 2)^{1/2}, \quad (1)$$

where λ and G are wavelength and the gap between the X-ray absorber and the PMMA resist. In order to fabricate sub-micron microstructures, the values of λ and G must be reduced.

In our experiment, deep X-ray lithography is carried out using the LIGA beamline of the synchrotron radiation (SR) light source, "AURORA", at Ritsumeikan Univer-

sity. The beamline is composed of a 200 μm thick layer of Be and a 50 μm thick layer of Kapton as band-pass filters. Critical wavelength and wavelength range at the beamline are 0.4 nm and from 0.15 nm to 0.8 nm [6]. The Fresnel diffraction and photoelectrons from the wavelength range have the smallest influence on X-ray lithography resolution [5]. Therefore, the gap must be controlled precisely in order to fabricate the sub-micron microstructures. Figure 1 shows the influence of Fresnel diffraction on resolution under different gaps at $\lambda=0.4$ nm. It was found that the gap must be set at less than 0.2 μm for sub-micron deep X-ray lithography.

On the other hand, the influence of the creation of photoelectrons will be increased at shorter wavelengths. However, it has been reported that the creation of photoelectrons did not influence the accuracy of the X-ray lithography [7].

FABRICATION

X-Ray Mask Design

Figure 2 shows an X-ray mask for deep X-ray lithography, composed of an X-ray absorber, a membrane and a frame. Table 1 shows the important requirements for the X-ray mask. Based on these requirements, Au, SiC and Si were selected as the X-ray absorber, the membrane and the frame respectively. The thicknesses of SiC and Si were decided at 2 μm and 625 μm . The required thickness of Au X-ray absorbers was decided in the following procedure.

A beam spectrum from AURORA is converted into an X-ray energy spectrum, e_0 , per unit time. Exposure energy, E , at the terminal of the beamline for LIGA is given by

$$E = \int e d\lambda = \int [e_0 \times \exp\{-(x_{Be}\mu_{Be} + x_{Ka}\mu_{Ka})\}] d\lambda, \quad (2)$$

where e is the spectrum of X-ray energy at the terminal of the beamline. x_{Be} (μm) and x_{Ka} (μm) are the thickness of Be and Kapton, which are 200 μm and 50 μm respectively. μ_{Be} (μm^{-1}) and μ_{Ka} (μm^{-1}) are the absorption coefficients of Be and Kapton. Transmitted energies of the X-rays through the membrane, E_M , and through the absorber, E_A , can be expressed as

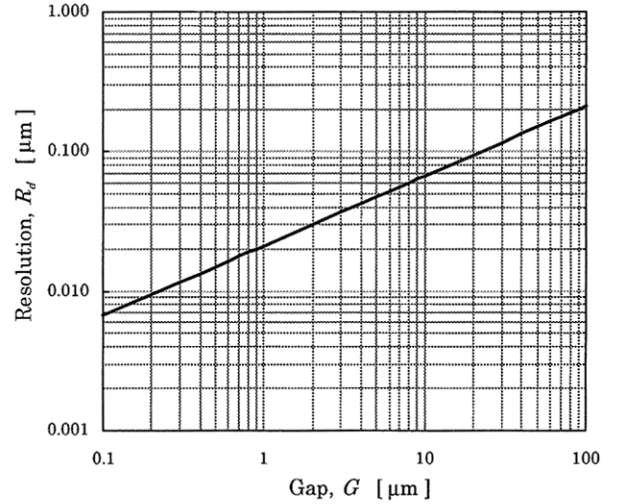


Figure 1: Influence of Fresnel diffraction on resolution.

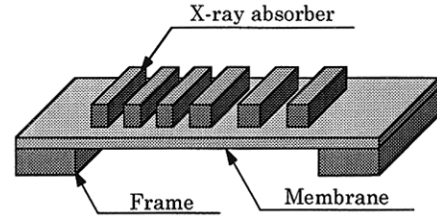


Figure 2: Structure of an X-ray mask for deep X-ray lithography.

Table 1: Important requirements for an X-ray mask for deep X-ray lithography.

X-ray absorber
high absorption against X-rays
high accuracy of the pattern
Membrane
high transparency against X-rays
high optical transparency
moderate tensile stress
high Young's modulus
Frame
high mechanical strength

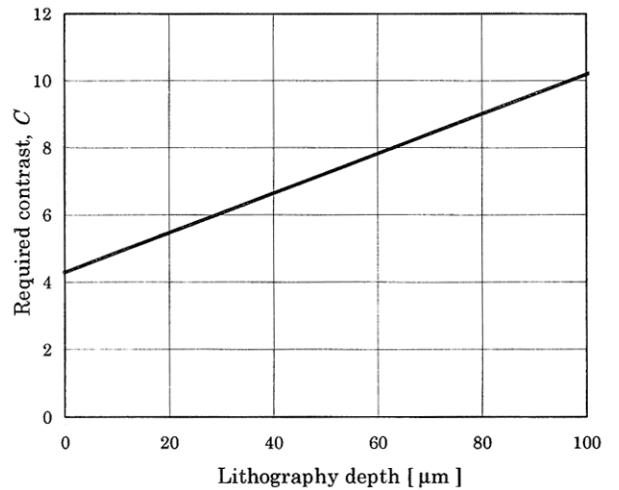


Figure 3: Required contrast, C , versus lithography depth.

$$E_M = \int [e \times \exp(-x_{SiC} \mu_{SiC})] d\lambda, \quad (3)$$

$$E_A = \int [e \times \exp\{-(x_{SiC} \mu_{SiC} + x_{Au} \mu_{Au})\}] d\lambda, \quad (4)$$

where x_{SiC} (μm) and x_{Au} (μm) are the thicknesses of SiC and Au. μ_{SiC} (μm^{-1}) and μ_{Au} (μm^{-1}) are the absorption coefficients of SiC and Au. Contrast, C , is defined as the ratio of E_M to E_A ;

$$C = \frac{E_M}{E_A}. \quad (5)$$

In order to fabricate microstructures with a high aspect ratio, a large value of C is required. Figure 3 shows the required contrast, C , versus a lithography depth using the X-ray mask with a SiC membrane of $2 \mu\text{m}$ thickness. This result shows that C is required to be 5.5 for X-ray lithography of a $20 \mu\text{m}$ thick PMMA resist. Figure 4 shows the required Au thickness versus a lithography depth using the X-ray mask. It was found that an Au X-ray absorber of $1 \mu\text{m}$ thickness was necessary for deep X-ray lithography of $20 \mu\text{m}$ thick PMMA.

X-Ray Mask Fabrication

In sub-micron deep X-ray lithography, one of the most crucial considerations is the fabrication of an X-ray mask with thick X-ray absorbers. The designed X-ray mask is composed of $1 \mu\text{m}$ thick Au as an X-ray absorber, $2 \mu\text{m}$ thick SiC as a membrane and $625 \mu\text{m}$ thick Si as a frame. The combination of the absorber of $1 \mu\text{m}$ thick Au and the membrane of $2 \mu\text{m}$ thick SiC gives a contrast of about 5.5 which is required for deep X-ray lithography of a $20 \mu\text{m}$ thick PMMA resist using the energy spectrum produced by AURORA.

Figure 5 shows a procedure for a fabrication process of an X-ray mask with Au absorbers having sub-micron widths and gaps. This fabrication process was adopted as it is the procedure that obtains the smallest deformation of X-ray absorbers. After SiC etching on the reverse side by reactive ion etching (RIE), a membrane was formed by KOH etching (a). A metal seed layer for Au electroforming was formed on the upper side by vacuum evaporation (b). Sub-micron structures of electron beam (EB) resist as molds were formed by lithography using EB direct writing (c). After Au elec-

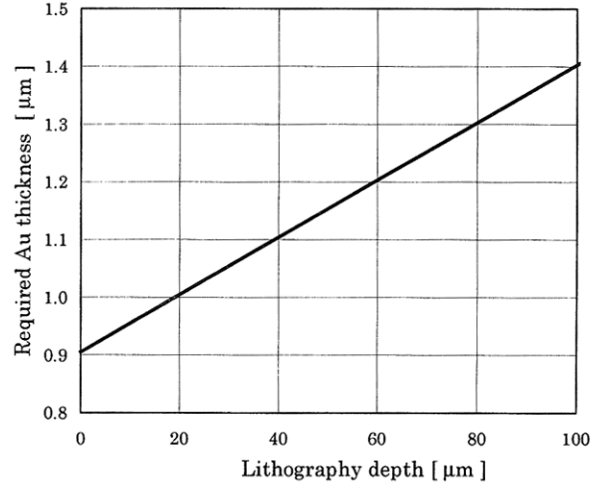


Figure 4: Required Au thickness versus lithography depth.

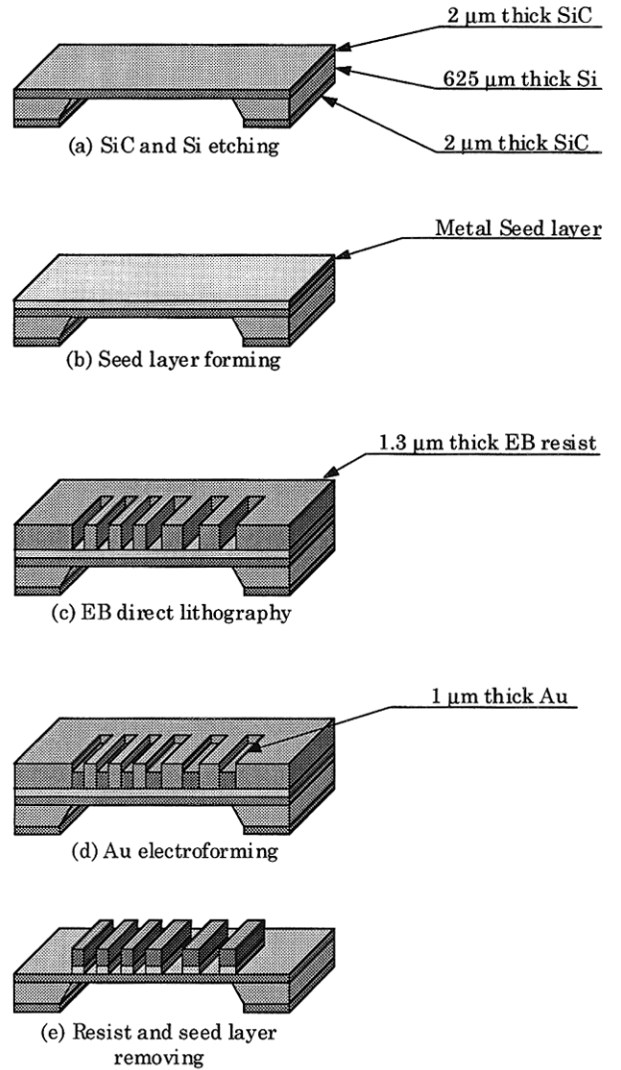


Figure 5: Procedure for fabrication process of an X-ray mask for sub-micron deep X-ray lithography.

troforming (d), the EB resist structures and the metal seed layer were removed by wet etching using an organic solution and an acid solution (e). Figure 6 shows an SEM photograph of fabricated X-ray absorbers with 0.6 μm lines width, 0.2 μm spaces, 1 μm thickness and a slope of about 84°. An X-ray mask with a maximum membrane size of 60 mm \times 30 mm can be fabricated. The membrane stress is 240 MPa of tensile stress.

Resist Forming

As shown in Fig.1, the gap between the X-ray mask and the PMMA resist must be set at less than 0.2 μm . However, there is a problem where a warp forms in a sample of a PMMA resist on a Si substrate by reason of residual stress which is generated by a high polymerization temperature and a difference of thermal expansion coefficients between Si ($3.6 \times 10^{-6} / ^\circ\text{C}$) and PMMA ($75.0 \times 10^{-6} / ^\circ\text{C}$).

A curvature radius, κ , of the warp in the sample and residual stress of the PMMA resist, σ_P , are given by

$$\frac{1}{\kappa} = \frac{(E_P t_P^3 + E_{Si} t_{Si}^3)(E_P t_P + E_{Si} t_{Si})}{6E_P E_{Si} t_P t_{Si} (\alpha_P - \alpha_{Si}) \times \Delta T} + \frac{3E_P E_{Si} t_P t_{Si}^2}{6E_P E_{Si} t_P t_{Si} (\alpha_P - \alpha_{Si}) \times \Delta T}, \quad (6)$$

$$\sigma_P \cong -\frac{E_P t_P^3 + E_{Si} t_{Si}^3}{6t_P t} \times \kappa, \quad (7)$$

where E_P and E_{Si} are Young's modulus of PMMA and Si, t is the total thickness of Si and PMMA resist, t_P and t_{Si} are the thickness of PMMA resist and Si, α_P and α_{Si} are the thermal expansion coefficients of PMMA and Si, and ΔT is temperature change.

Figure 7 shows the residual stress of PMMA versus different polymerization temperatures. These experimental values are similar to the calculated results. Based on these results, by controlling the temperature of the polymerization process, a PMMA resist was polymerized without residual stress, which was the main cause of the warp in the sample.

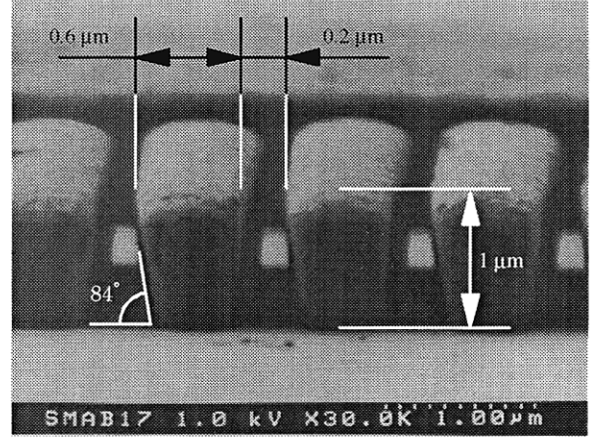


Figure 6: SEM photograph of sub-micron X-ray absorbers fabricated by Au electroforming after lithography using EB direct writing.

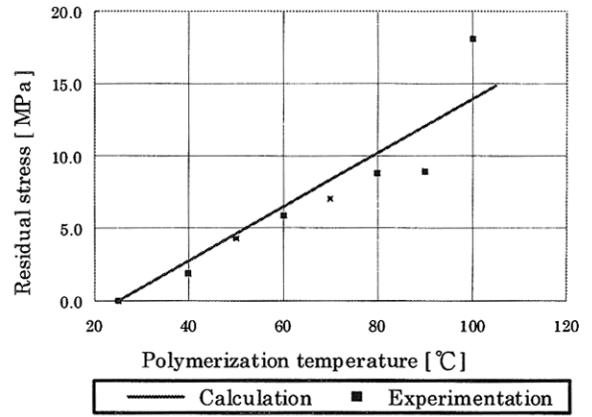


Figure 7: Residual stress of PMMA versus different polymerization temperatures.

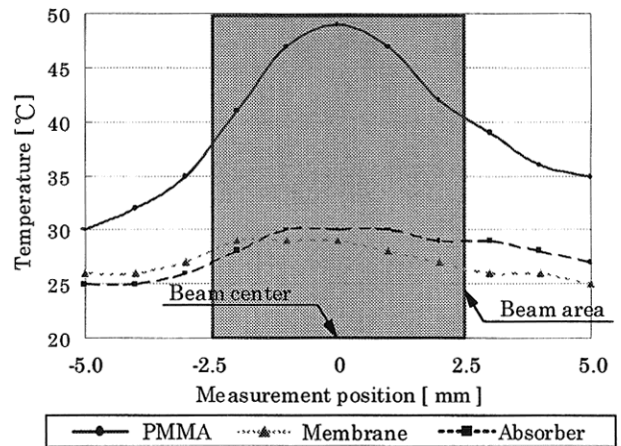


Figure 8: Surface temperature profiles of a PMMA resist, a SiC membrane and an Au absorber under SR X-ray irradiation.

Lithography

In order to fabricate sub-micron structures, the deformation of the X-ray absorber, the membrane and the resist due to heat generation under SR X-ray irradiation must be taken into consideration. Figure 8 shows the profiles of the surface temperature of a PMMA resist, a SiC membrane and an Au X-ray absorber in He at 1 atm under SR X-ray irradiation. The surface temperature of the PMMA resist indicated an increase of 25 °C. In calculation, the maximum stress of the PMMA resist is a compressive stress of 6 MPa. This stress may be the main cause of a warp in the sample and deformation of the PMMA resist. However, this stress can be reduced by repetition of short time exposure or cooling down the sample. On the other hand, an increase of 5 °C of the surface temperature of the Au X-ray absorber and the SiC membrane was indicated. In calculation, the maximum stress of the Au X-ray absorber and the SiC membrane is a compressive stress of 5 MPa. However, this is not a problem as the stress is compensated by the tensile stress of 240 MPa in the SiC membrane.

RESULTS AND DISCUSSION

Figure 9 shows PMMA structures with sub-micron width fabricated by deep X-ray lithography under the following conditions: an exposure gap between X-ray mask and resist surface of 60 μm and an exposure dose of 9 mA min / mm^2 . As shown in Fig. 10, a PMMA structure, which has a 0.2 μm minimum width, 6 μm maximum length and 17 μm height, was fabricated.

One of the important factors in evaluating fabricated microstructures with high aspect ratio is taper ratio. As shown in Fig. 11, the microstructure has a taper ratio of 0.168 / 100. Moreover, as shown in Fig. 12, the top and bottom parts of the microstructure deviate from the vertical. In the top part, it is thought that the deviation of 0.17 μm has been influenced by Fresnel diffraction because the value of the deviation gave good agreement with the value obtained by Eq. (1). In the bottom part, it is thought that the deviation of 0.15 μm has been influenced by secondary electrons from the substrate and the seed layer [8]. In order to reduce the influence of

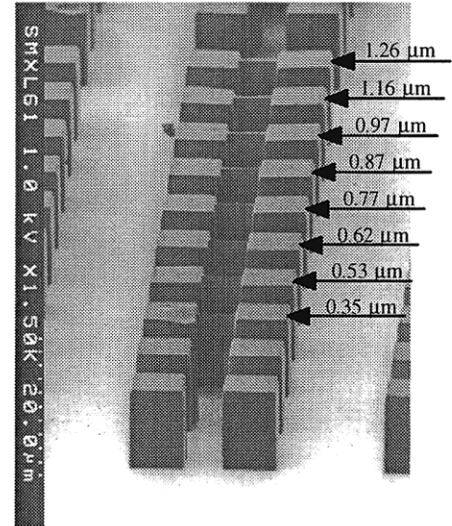


Figure 9: SEM photograph of sub-micron PMMA structures fabricated by deep X-ray lithography.

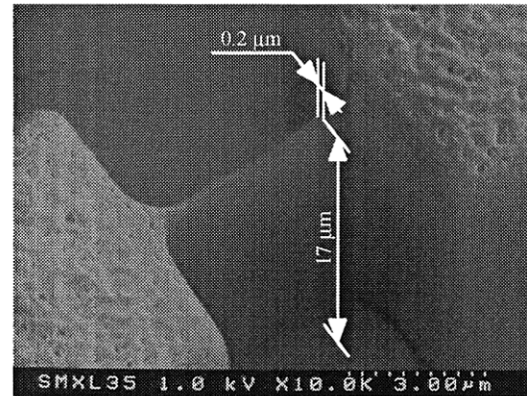


Figure 10: SEM photograph of a sub-micron PMMA structure with 0.2 μm minimum line width.

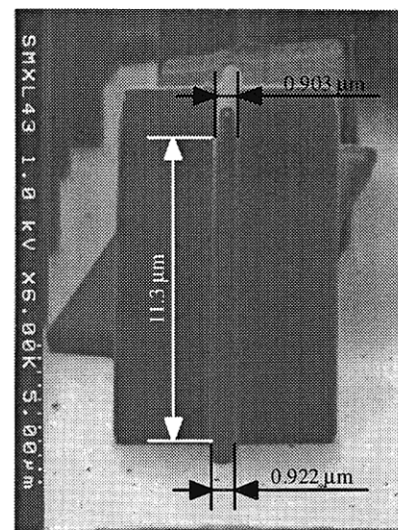


Figure 11: SEM photograph of a PMMA structure with a taper ratio of 0.168/100.

secondary electrons, it might be necessary to select an element with a lower atomic number for the substrate and the seed layer.

CONCLUSIONS

An X-ray mask, which is composed of 1 μm thick Au as absorbers, 2 μm thick SiC as a membrane and 625 μm thick Si as a frame, was fabricated. A fabrication process which obtains the smallest deformation of X-ray absorbers of the X-ray mask, was adopted. The X-ray mask has X-ray absorbers with sub-micron lines and spaces. The membrane stress of the X-ray mask is 240 MPa of tensile stress, which compensates the stress caused by heat generation under SR X-ray irradiation. By controlling the polymerization process the PMMA resist was polymerized without residual stress, which was the main cause of a warp in a sample of a PMMA resist on a Si substrate. Therefore Fresnel diffraction had less influence on the accuracy of the deep X-ray lithography. As a result, a sub-micron PMMA structure with 0.2 μm minimum width, 6 μm length and 17 μm height was fabricated by deep X-ray lithography.

These results are expected to be applicable to the manufacturing of practical and high performance MEMS devices. In particular, sub-micron PMMA structures fabricated by deep X-ray lithography are expected to be applicable to optical communication devices because PMMA is characterized by a high permeability to visible light. In future work, we intend to develop optimum conditions of sub-micron deep X-ray lithography and to fabricate practical and high performance MEMS devices.

ACKNOWLEDGEMENT

The authors would like to thank A. Kurikawa and H. Horiuchi at HOYA Corporation for supplying of SiC substrates.

REFERENCES

- [1] Hiroshi Ueno, Makoto Hosaka, Osamu Tabata, Satoshi Konishi and Susumu Sugiyama, "X-ray Mask with SiC Membrane for LIGA Process", T. IEE Japan, 119-E, 4, 1999, pp. 229-235.
- [2] Ryoji Kondo, Shinsuke Takimoto, Kenichiro Suzuki and Susumu

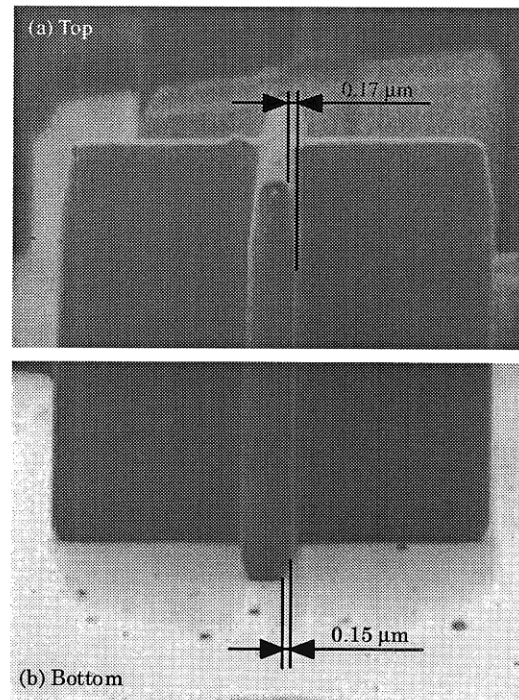


Figure 12: SEM photographs of top and bottom parts of PMMA structures fabricated by sub-micron deep X-ray lithography.

- Sugiyama, "High Aspect Ratio Electrostatic Micro Actuators Using LIGA Process", HARMST'99, 1999, pp.138-139.
- [3] M. W. Borner, M. Kohl, F.J. Pantenburg, W. Bacher, H. Hein, and W.K. Schomburg, "Sub-Micron LIGA Process for Movable Microstructures", Microelectronic Engineering, 30, 1996, pp. 505-508.
- [4] A. Azzam Yasseen, Chein-Hung Wu, Christian A. Zorman, and Mehran Mehregany, "Fabrication and Testing of Surface Micro-machined Silicon Carbide Micromotors", MEMS'99, 1999, pp. 644-649.
- [5] W. Ehrfeld and H. Lehr, "Deep X-ray Lithography for the Production of three-dimensional Microstructures from Metals", Polymers and Ceramics: Radiation Phys. Chem., Vol.45, 1995, pp. 349-365.
- [6] S. Sugiyama, Y. Zhang, H. Ueno, M. Hosaka, T. Fujimoto, R. Maeda and T. Tanaka, "A Compact SR beamline for Fabrication of High Aspect Ratio MEMS Microparts", MHS'96, 1996, pp. 79-84.
- [7] P. Bley and J. Mohr, "The LIGA Process -A Microfabrication Technology-", FED Journal Vol.5 Suppl. 1, 1994, pp. 34-48.
- [8] A. Schmidt, A. Clifton, W. Ehrfeld, G. Feiertag, H. Lehr, M. Schmidt, "Investigation of the Adhesive Strength of PMMA Structures on Substrates obtained by Deep X-ray Lithography", Microelectronic Engineering 30, 1996, pp. 215-218.